J. Fluid Mech. (1983), *vol.* 133, *pp.* 245–254
Printed in Great Britain

An experimental study of gas exchange in laminar oscillatory flow

By C. H. JOSHI, R. D. KAMM,
Massachusetts Institute of Technology, Cambridge, MA 02139

J. M. DRAZEN
Brigham and Women's Hospital, Boston, MA 02115

AND A. S. SLUTSKY
West Roxbury V.A. Medical Center, Boston, MA 02132

(Received 13 July 1982 and in revised form 20 February 1983)

Experiments were conducted to determine the effective diffusivity for axial transport through a tube of circular cross-section of a contaminant gas in oscillatory flow. Results were compared with the theoretical predictions of Watson (1983) and found to be in excellent agreement. The experiments differ from the theoretical situation in that the oscillations are superimposed upon a steady flow due to a constant infusion of tracer gas, and a buoyancy-induced flow associated with spatial variations in gas density. The influence of both artifacts is found to be negligible.

1. Introduction

Numerous studies have been conducted of axial dispersion in steady, laminar flow within a tube of uniform, circular cross-section (e.g. Taylor 1953; Aris 1956). The theoretical results obtained from these investigations have demonstrated that, as time progresses, a concentration non-uniformity spreads over an increasing axial distance at a rate which depends upon both axial convection and radial molecular diffusion. This combination of transport mechanisms is termed 'augmented diffusion'. As the term implies, the rate of axial transport is greater than would be expected from molecular diffusion alone. By contrast, however, radial molecular diffusion acts to *reduce* the net rate of dispersion from that which would occur in a fluid mixture having zero molecular diffusivity, owing to migration of the dispersing species between the region of rapid fluid motion near the tube centreline and the slow-moving regions near the wall. Consequently, the dispersion observed in steady flow could also be described as 'diffusion-limited convective transport'.

The analytical results for augmented diffusion in steady flow can be cast in the form of an effective axial diffusion coefficient K, which, for times long compared with the time for radial molecular diffusion, has the form (Aris 1956):

$$K = \kappa(1+R_s), \tag{1}$$

where R_s has been shown by Taylor (1953) to be

$$R_s = \frac{1}{48}\frac{\bar{u}_s^2 a^2}{\kappa^2}.$$

Here $\bar{u}_s$ is the steady cross-sectional average velocity, κ is the molecular diffusion coefficient and a is the tube radius. The symbol R_s is used to represent the component transport due to augmentation by convection in steady flow.

Shear-augmented axial dispersion in oscillatory flows has been investigated for a variety of circumstances by Bowden (1965), Holley, Harleman & Fischer (1970) and Chatwin (1970) among others. The particular instance of these experiments is analysed in the companion paper (Watson 1983). The convective and diffusive mechanisms are the same as in steady flow, but the overall results differ very significantly. For example, if the oscillation period is large compared with the transverse mixing time, then the dispersion can be much less efficient than in an otherwise equivalent steady flow owing to the perfect directional symmetry in the velocity profile (see e.g. Holley *et al.* 1970; Smith 1982). The steady and oscillatory flows are inherently different in this respect. Conversely, in the presence of radial molecular diffusion, net transport does occur by virtue of the radial exchange of material between adjacent streamlines. As the radial diffusion time becomes small compared with the cycle period, a quasisteady situation results in which the instantaneous dispersion can be predicted by the steady-flow result (Chatwin 1975). By this line of reasoning it can be seen that the augmentation of dispersion approaches zero for both very high and very low values of an appropriately defined dimensionless frequency if all other conditions are held constant.

In this paper, we report the results of an experimental study of gas exchange in laminar oscillatory flow. Motivation for this study is provided by the possible importance of augmented diffusion to pulmonary ventilation by high-frequency low-volume oscillations (Slutsky *et al.* 1980). Although the details of gas exchange in the branching airways of the lung certainly differ from those in a long, uniform-diameter tube, mechanisms of a similar nature are likely to be important in the small airways where flow is laminar and secondary flows are minimal.

Watson (1983) has shown that, in a long tube of uniform cross-section, the time-mean flux of some fluid constituent across a stationary cross-sectional plane is given by

$$\bar{q}_c = -K\frac{d\bar{\theta}}{dx}, \tag{2}$$

where $\bar{\theta}$ is the time-mean cross-sectional average concentration and K now represents the effective axial diffusion coefficient for oscillatory flow, which has the form given below in (11). This relationship strictly applies only for the case of purely oscillatory flow in an infinitely long tube with steady boundary conditions, and sufficiently long after the onset of dispersion so that the axial gradient of $\bar{\theta}$ is nearly linear (Smith 1982; Allen 1981). For example, after introduction of a contaminant species into an oscillatory flow, the result applies in a local region for times greater than that required for diffusion over the entire cross-section of the tube (of order a^2/κ).

2. Description of the experiments

2.1. *Experimental rationale*

The experiments were conducted using a tube of circular cross-section, long enough to avoid significant end effects in the mid-region, even at the largest stroke volumes employed.

To ensure that the flow was laminar, the experimental combinations of stroke volume and frequency were chosen so that the relevant dimensionless parameter Re/α (where $Re = 2\hat{u}a/\nu$ and $\alpha = a(\omega/\nu)^{\frac{1}{2}}$; $\hat{u}$ is the root-mean-square spatially averaged

velocity, ν the kinematic viscosity of the fluid mixture and ω the angular frequency of oscillation) was less than the critical value for transition to turbulence found by Merkli & Thomann (1975) and Sergeev (1966) of from 250 to 500. For large α, Re/α is the Reynolds number based on viscous boundary-layer thickness inasmuch as α is a measure of the ratio of tube diameter to boundary-layer thickness.

Measurements were made during a steady-state gas-exchange process in which the time mean of all variables, over an integer number of cycles, remained constant. To this end, a tracer gas was introduced at a constant rate of infusion at one end of the tube, thus providing a minute volume flow passing steadily through the tube, on top of which was superimposed the flow oscillations. The opposite end of the tube was open to room air, and therefore maintained at nearly zero concentration of the contaminant gas. The transport of tracer at any axial position was therefore due to a combination of convection owing to the bulk flow, and augmented diffusion.

The time required to achieve this steady-state condition of constant time-mean tracer flux at all axial locations is much greater than the short-term requirement stated earlier ($t \approx a^2/\kappa$), and is estimated to be of order L^2/K, where L is the length of the tube. For the smallest values of K observed in these experiments, approximately 20 hours were required to reach a state of steady axial transport.

This situation differs slightly from that analysed by Watson owing to the steady-flow component. To consider the influence of the mean flow, we divide the velocity and concentration into two components, one representing the mean value, over one oscillation period, of the cross-sectional average, the other representing perturbations upon this mean value. Thus, velocity u and concentration θ can be expressed as

$$u(X,t) = \bar{u}(x) + u'(X,t), \tag{3a}$$

$$\theta(X,t) = \bar{\theta}(x) + \theta'(X,t), \tag{3b}$$

where $X = (x, y, z)$, and barred quantities are defined by

$$\bar{\phi} \equiv \frac{1}{AT}\int_0^A \int_0^T \phi \, \mathrm{d}t \, \mathrm{d}A.$$

Here T is the oscillation period and A the tube cross-sectional area. The instantaneous species volume flux in the axial direction can then be written

$$\begin{aligned} q_c &= u\theta - \kappa \frac{\partial \theta}{\partial x} \\ &= \bar{u}\bar{\theta} + \bar{u}\theta' + u'\bar{\theta} + u'\theta' - \kappa \frac{\partial \theta}{\partial x}. \end{aligned} \tag{4}$$

Integrating over the tube cross-section and over an oscillation period yields

$$\bar{q}_c = \bar{u}\bar{\theta} + \overline{u'\theta'} - \kappa \frac{\mathrm{d}\bar{\theta}}{\mathrm{d}x}, \tag{5}$$

which differs from the form produced by Watson by the appearance of the first term on the right-hand side. It has been shown in a variety of circumstances (e.g. Taylor 1953) that the second term on the right can be simplified by introducing an effective diffusivity K to give

$$\bar{q}_c = \bar{u}\bar{\theta} - K \frac{\mathrm{d}\bar{\theta}}{\mathrm{d}x}. \tag{6}$$

Since the analysis of Watson is valid regardless of how the flow varies with time, this step is justified even in the presence of a steady flow as due, for example, to the

slow infusion of trace gas in the experiments. The additional effects of buoyancy-induced flow (both axial and in the cross-sectional plane) have been considered in combination with steady flow by Erdogan & Chatwin (1967) and can be shown to be negligible in these experiments.

Since both $\bar{u}$ and $\bar{q}_c$ are equal to the volume flux of pure contaminant at the point of infusion, $\bar{q}_{c0}$, the concentration profile obtained by integrating (6), can be written

$$\bar{\theta} = 1-(1-\bar{\theta}_1)\exp\left[\frac{\bar{q}_{c0}}{K}(x-x_1)\right], \tag{7}$$

where x_1 is a point of known concentration $\bar{\theta}_1$. Rearranging (7) we obtain an expression for K in terms of the measured concentrations at two points x_1 and x_2:

$$K = \bar{q}_{c0}(x_1-x_2)\ln\frac{1-\bar{\theta}_1}{1-\bar{\theta}_2}. \tag{8}$$

Thus by measuring the concentration of contaminant at two positions, an experimental value for K can be determined.

The values of concentration $\bar{\theta}_1$ and $\bar{\theta}_2$ are cross-sectional- and time-averaged quantities, and as such are difficult to measure directly without disrupting the flow. For the purpose of making a non-invasive measurement, an infrared-absorption technique was selected. A collimated laser beam was directed along a tube diameter and detected on the opposite side. Methane ($\kappa \approx 0.17$ cm^2/s), having a strong absorption band coincident with the laser emission, was used as the contaminant gas.

Measurements made in this fashion give an instantaneous diametral-average concentration, which, for a non-uniform concentration profile, differs from the cross-sectional average. To determine the potential error, we used the theoretical result of Watson (1983) to compute the concentration profiles during different phases of the oscillation cycle. In the worst case (the largest values of concentration gradient and stroke volume used in the experiments) the error introduced by taking the diametral average rather than the area average was determined to be less than 5 %.

2.2. *Experimental apparatus*

Our measurements were made using the apparatus shown schematically in figure 1. Flow oscillations were produced by a motor-and-crank assembly driving a low-friction graphite piston within a glass cylinder. The tube connecting the piston cylinder to the test section contained a gradually tapered duct to provide a smooth transition between the piston and tube cross-sectional areas. At this point the tracer gas was infused first into an outer plenum and then through numerous perforations in the wall of the tube to distribute the tracer gas uniformly around the circumference. The tracer flow was produced by a syringe pump, which was calibrated to give an accuracy of 0.5 % and a repeatability of 0.1 % over the range from 0.5 ml/h to 3.0 ml/s.

The tube in which our measurements were made was 1.2 m in length with an inner diameter of 10 mm. A quartz tube was used to minimize attenuation of the laser beam. The end of the tube opened to stagnant room air.

Concentrations were determined by measuring the intensity decrement of a 5 mW He–Ne laser beam (wavelength = 3.39 μm) directed along the tube diameter perpendicular to the tube axis. Using Beer's law, the diametral-average concentration can be found from the expression

$$\bar{\theta} \approx \frac{1}{2a}\int_{-a}^{a}\theta\,\mathrm{d}r = \frac{1}{2a\beta}\ln\left(\frac{I_1}{I_0}\frac{I_0}{I}\right) \tag{9}$$

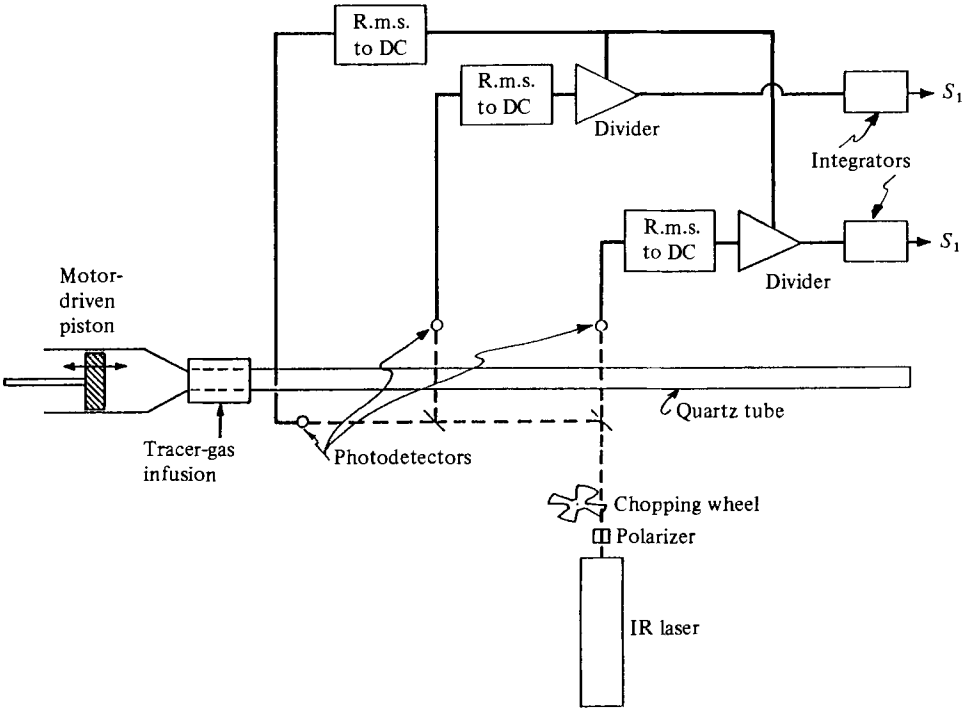

FIGURE 1. Experimental apparatus with signal-conditioning components.

where $\hat{\beta}$ is the methane absorption coefficient ($\hat{\beta} = 9.0$ cm^{-1} atm^{-1}), I_0 is the intensity of the reference beam, I_1 is the intensity of the beam passing through the tube when no tracer gas is present, and I is the measured intensity with tracer gas present. The intensities are left in terms of ratios to a reference beam (produced at a beam splitter prior to entering the quartz tube) to compensate for fluctuations in the laser output.

For the purpose of measurement by the infrared detectors (Pb–Se) the beam was chopped at a frequency of 1200 Hz. Also, the beam was plane polarized upon exiting from the laser. This was necessary because it was found that changes in polarization caused the ratio of reflected to transmitted beam intensity from a beam splitter to vary by substantial amounts. With polarization, fluctuations in the ratio I_0/I_1 were kept below 2%.

Radiation reaching the detector produced a voltage output proportional to the beam intensity which was processed in the manner shown in figure 1. First the oscillatory outputs from each detector were amplified and converted from AC to DC using an Analog Devices RMS/DC Converter. The intensity ratios of (9) were then determined by dividing the DC signal from either of the two measurement detectors by the reference signal (using an Analog Devices 2-Quadrant Signal Divider). These signals were integrated over a 20–40 s interval to yield time averages. Equation (9) was then used to compute $\bar{\theta}$.

Prior to each experiment, the methane flow rate was selected so as to produce a methane concentration of about 10% at the two measurement locations. Concentrations much below 10% did not allow for adequate discrimination between the two points of measurement. The ratio of peak oscillatory flow amplitude to steady flow amplitude ranged from 6×10^2 to over 3×10^3. After a steady state had been reached

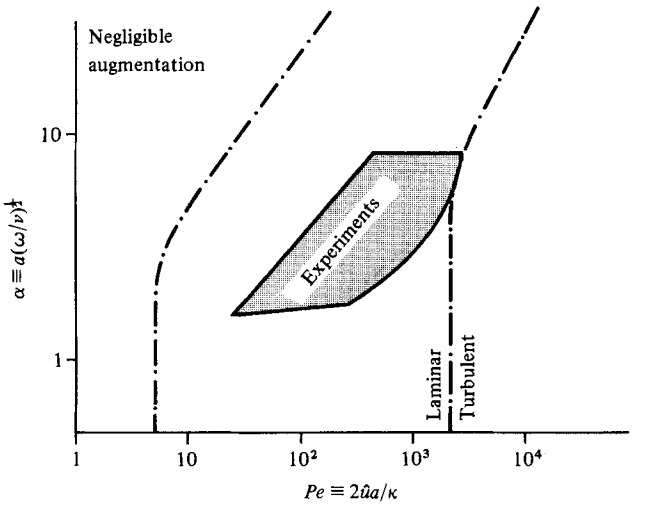

FIGURE 2. A mapping of the range of experiments. The extended 'laminar–turbulent' transition line is for $\sigma \equiv \nu/\kappa = 1$. For low α, the transition line is based on the root-mean-square velocity.

during tracer infusion at a constant rate, concentrations were measured at two locations 24 cm apart, located near the centre of the quartz tube. These concentrations are related to the effective diffusivity through (8). Since all parameters on the right-hand side of (8) are known or can be measured, we can solve for K.

In figure 2 the range of our experiments is mapped in terms of Péclet number $Pe = 2\hat{u}a/\kappa$ and Womersley number α. Shown also is the range where augmentation is negligible ($K/\kappa - 1 < 0.1$) and the estimated locus of transition from laminar to turbulent flow, assuming $\sigma = \nu/\kappa = 1$. To form the approximate line of transition we used the experimental results of Merkli & Thomann (1975) and Sergeev (1966) for high α, and assumed that, for low α, the critical Reynolds number (based on peak velocity) approaches the steady-flow value of about 2300.

3. Results and discussion

Experiments were systematically performed for discrete stroke volumes and for a range of frequencies covering the region mapped out in figure 2. The results are plotted in three ways. In figure 3, K/κ is plotted against a dimensionless stroke volume V^2/a^6, where V is the stroke volume of oscillation. These tests were all conducted at a single frequency corresponding to $\alpha = 7.33$. For comparison, it is helpful to express the theoretical result in the form

$$\frac{K}{\kappa} = 1 + h(\alpha, \sigma)\frac{V^2}{a^6}, \tag{10}$$

where

$$h(\alpha, \sigma) = \frac{\alpha^3}{4\pi^2(1-\sigma^{-2})} \frac{T_3(\alpha) - \dfrac{T_2(\alpha)\,T_3(\beta)}{\sigma^{\frac{1}{2}}T_2(\beta)}}{\alpha^2 T_1(\alpha) - 4\alpha T_4(\alpha) + 4T_2(\alpha)},$$

$$T_1(\xi) = \mathrm{ber}^2\xi + \mathrm{bei}^2\xi,$$

$$T_2(\xi) = (\mathrm{ber}'\xi)^2 + (\mathrm{bei}'\xi)^2,$$

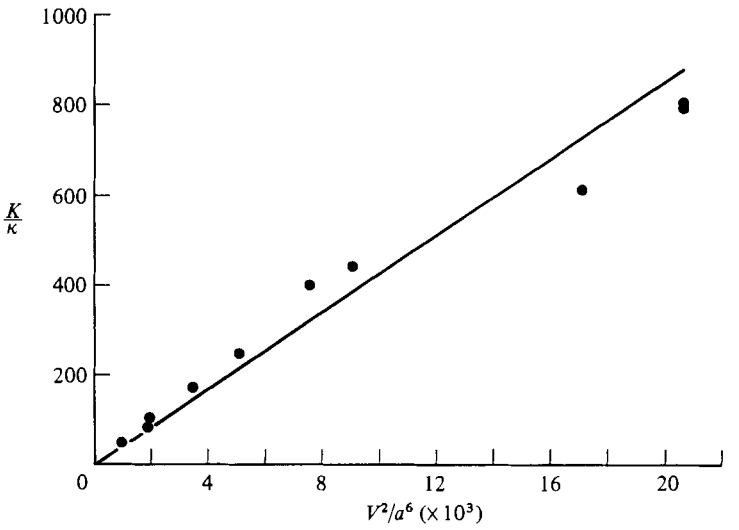

FIGURE 3. Results for one series of tests in which the frequency was held constant while the stroke volume was varied. The six points (superimposed) at $V^2/a^6 = 2.02 \times 10^4$ and the two points at $V^2/a^6 = 3380$ were obtained for a range of methane flow rates (see text). Solid line, theoretical predictions for corresponding values of V^2/a^6, (10).

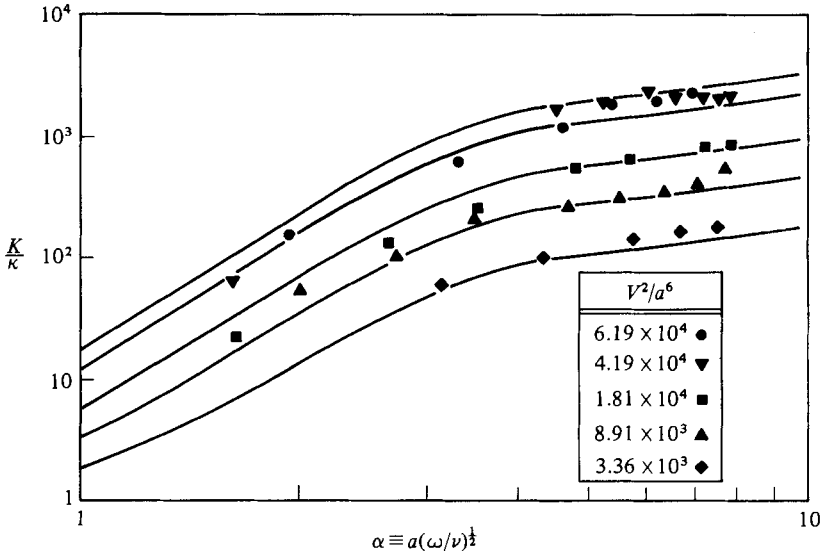

FIGURE 4. Results for several test sequences in which the stroke volume was held constant while the oscillation frequency was varied. Solid lines, theoretical prediction, (10).

$$T_3(\xi) = \mathrm{ber}\,\xi\,\mathrm{ber}'\xi + \mathrm{bei}\,\xi\,\mathrm{bei}'\xi,$$

$$T_4(\xi) = \mathrm{ber}\,\xi\,\mathrm{bei}'\xi - \mathrm{ber}'\xi\,\mathrm{bei}\,\xi,$$

$$\beta \equiv \alpha\sigma^{\frac{1}{2}},$$

and where ber and bei are defined in relation to the Bessel function I_0 by

$$I_0(\xi i^{\frac{1}{2}}) = \mathrm{ber}\,\xi + \mathrm{i}\,\mathrm{bei}\,\xi.$$

To test the effect of methane flow rate, six experiments were conducted at $V^2/a^6 = 2.02 \times 10^4$, each with a different methane flow rate ranging from 0.0107 to 0.187 ml/s. Two tests were run at $V^2/a^6 = 3380$ with methane flow rates of 1.53×10^{-3} and 9.2×10^{-3} ml/s. Both sets of repeated tests proved to be highly reproducible, supporting our claim that these minute steady flow rates have no significant influence over the measured diffusivities.

Figure 4 shows K/κ plotted as a function of α for each of several values of a dimensionless stroke volume. In this graph, each curve represents one set of experimental data where the experimental conditions were changed merely by changing the frequency of oscillation.† As exhibited by (10), when V^2/a^6 is held constant K/κ varies as α in the limit of high frequency, and approaches unity for small frequencies as $h(\alpha)$ goes to zero. The theory, indicated by the solid curves, shows these high- and low-frequency limits connected by a transition region.

In each of the curves of figure 4, the highest values of Reynolds number and Re/α are found at the right-hand edge of the plot. In spite of values of Re/α as high as 300 (for $V^2/a^6 = 6.19 \times 10^4$), there appears to be no effect on axial transport due to turbulence or transitional flow. With the present apparatus we were unable to extend the range of experiments to sufficiently high stroke volumes or frequencies to further explore the transition to turbulence.

Another useful way to view the data is suggested by the following variation on (10):

$$\frac{K}{\kappa} = 1 + f(\alpha, \sigma)\, Pe^2, \tag{11}$$

where

$$f(\alpha, \sigma) = \frac{1}{2\alpha(\sigma^2-1)} \frac{T_3(\alpha) - \dfrac{T_2(\alpha)\, T_3(\beta)}{\sigma^{\frac{1}{2}} T_2(\beta)}}{\alpha^2 T_1(\alpha) - 4\alpha T_4(\alpha) + 4T_2(\alpha)}.$$

For experiments conducted using a single tracer gas, σ is constant. $f(\alpha, \sigma)$ is then a function only of the dimensionless frequency. Plotting $(K/\kappa - 1)/Pe^2$ versus α yields a single curve, as demonstrated in figure 5, which contains all the data from figures 3 and 4. The high- and low-frequency limits for $\sigma \equiv 1$ can be written as

$$f(\alpha, 1) = \frac{1}{192} \quad (\alpha \lesssim 1),$$

$$f(\alpha, 1) = \frac{\alpha + 3\sqrt{\frac{1}{2}}}{8\sqrt{2}\,\alpha^4} \quad (\alpha \gg 1).$$

Note that, for low α, the constant coefficient agrees with the steady-flow result of Aris (1956).

In conclusion, the experiments are generally in good agreement with the theoretical

† For each test we took one of the two concentration measurements and the anticipated concentration profile (7), and extrapolated to find the location where the time-mean concentration would be zero. Comparing this estimate to the actual distance between the measurement location and the open end of the tube, we found large discrepancies in certain tests. We used this comparison to exclude tests which presumably had not achieved steady state owing either to premature termination or some disturbance during the test. Specifically, if the extrapolated distance differed by more than 25% from the anticipated value (estimated to be x_p to $x_p - V/A$ for high α, and x_p to $x_p - 2V/A$ for small α, where x_p is the measured distance from the detector location to the open end of the tube), that test was deemed invalid. Generally, the tests which were eliminated by this check were those which ran for extended periods of time before achieving steady state, sometimes as long as 20 h.

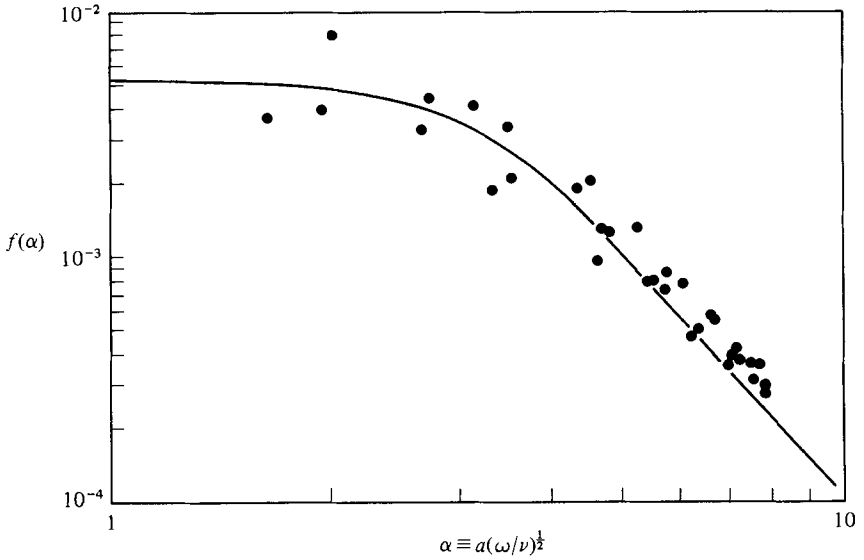

FIGURE 5. All the results from figures 3 and 4 plotted according to (11). Solid line, theoretical prediction.

predictions of Watson over a wide range of Re and α, for $\alpha = 1$. These results clearly demonstrate the rapid fall in the rate of axial dispersion as frequency increases at constant velocity amplitude. More recent results (Bullister 1983) confirm the trend indicated by the high-frequency limit following (11) up to values of α as high as 20.

That these experiments were performed with a steady component of flow apparently had little effect on the process of augmented diffusion, but had the considerable advantage of producing a steady-state exchange process in which measurements could be subjected to time averaging, thereby reducing experimental error.

The agreement obtained between these results and the theoretical predictions supports the use of these same experimental techniques in situations for which theoretical solutions are not available as in turbulent oscillatory flow and oscillatory flow through a bifurcating system.

The authors would like to acknowledge the assistance of Mark Minicelli, Gerald Mahoney and John Collins in the development of the experimental apparatus. This work was supported by grants from the National Institute of Health (HL 26566) and the National Science Foundation (CME-7913092).

REFERENCES

ALLEN, C. 1982 Numerical simulation of contaminant dispersion in estuary flows. *Proc. R. Soc. Lond.* **A381**, 179–194.

ARIS, R. 1956 On the dispersion of a solute in a fluid flowing through a tube. *Proc. R. Soc. Lond.* **A235**, 67–77.

BOWDEN, K. F. 1965 Horizontal mixing in the sea due to a shearing current. *J. Fluid Mech.* **21**, 83–95.

BULLISTER, E. T. 1983 Mass transfer in oscillatory flow under the influence of a turbulent jet. SM thesis, MIT.

CHATWIN, P. C. 1970 The approach to normality of the concentration distribution of a solute in a solvent flowing along a straight pipe. *J. Fluid Mech.* **43**, 321–352.

CHATWIN, P. C. 1975 On the longitudinal dispersion of passive contaminant in oscillatory flows in tubes. *J. Fluid Mech.* **71**, 513–527.

ERDOGAN, M. E. & CHATWIN, P. C. 1967 The effects of curvature and buoyancy on the laminar dispersion of solute in a horizontal tube. *J. Fluid Mech.* **29**, 465–484.

HOLLEY, E. R., HARLEMAN, D. R. & FISCHER, H. B. 1970 Dispersion in homogeneous estuary flow. *J. Hydraul Div. ASCE* **96** (HY8), 703–724.

MERKLI, P. & THOMANN, H. 1975 Transition to turbulence in oscillating pipe flow. *J. Fluid Mech.* **68**, 567–575.

SERGEEV, S. I. 1966 Fluid oscillations in pipes at moderate Reynolds numbers. *Fluid Dyn.* **1**, 121.

SLUTSKU, A., DRAZEN, J. M., INGRAM, R. H., KAMM, R. D., SHAPIRO, A. H., FREDBERG, J. J., LORING, S. H. & LEHR, J. 1980 Effective pulmonary ventilation with small-volume oscillations at high frequency. *Science* **209**, 609–611.

SMITH, R. 1982 Contaminant dispersion in oscillatory flows. *J. Fluid Mech.* **114**, 379–398.

TAYLOR, G. I. 1953 Dispersion of soluble matter in solvent flowing slowly through a tube. *Proc. R. Soc. Lond.* **A219**, 186–203.

WATSON, E. J. 1983 Diffusion in oscillatory pipe flow. *J. Fluid Mech.* **133**, 233–244.